PARAMETRIC STUDY OF RADIATIVE COOLING OF SOLID ANTIHYDROGEN

THESIS

Michael J. MacLachlan
Captain, USAF

AFIT/GNE/ENP/89M-4

DEPARTMENT OF THE AIR FORCE
AIR UNIVERSITY
AIR FORCE INSTITUTE OF TECHNOLOGY

Wright-Patterson Air Force Base, Ohio

AFIT/GNE/ENP/89M-4

PARAMETRIC STUDY OF RADIATIVE COOLING OF SOLID ANTIHYDROGEN

THESIS

Michael J. MacLachlan
Captain, USAF

AFIT/GNE/ENP/89M-4

Approved for public release; distribution unlimited

AFIT/GNE/ENP/89M-4

PARAMETRIC STUDY OF RADIATIVE COOLING OF SOLID ANTIHYDROGEN

THESIS

Presented to the Faculty of the School of Engineering

of the Air Force Institute of Technology

Air University

In Partial Fulfillment of the

Requirements for the Degree of

Master of Science in Nuclear Engineering

Michael J. MacLachlan, BM, BSEE

Captain, USAF

March 1989

Approved for public release; distribution unlimited

Preface

One expects to make discoveries as a result of research. In this project I discovered that a thesis is not something which sprouts like an acorn and grows slowly to maturity. This one grew more like a bacterial culture: ideas flourished, only to be proved wrong or irrelevant and be wiped out with electronic alacrity. Countless glorious inspirations have met their doom since I naively wrote my prospectus; in fact, I imagine no more than ten percent of even my "final" thesis draft is still included. It was fun, but I hope to imbue my next project with a little less of that sort of excitement.

The excitement could have been a killer if I hadn't had a lot of help. My thesis advisor, Lieutenant-Colonel Jim Lupo, saved me a lot of frustration. When I bogged down, he always had an answer. The other members of my committee, Captain Haaland and Major Beller, performed the invaluable if painful service of bringing me face to face with my many errors and lapses. Captain Steve Thompson of the Air Force Astronautics Laboratory was an indispensable source of information. I am also grateful to Captain Frank Turner for sharing his knowledge of things academic and otherwise.

Abstract

A computer model of a cryogenic system for storing solid antimatter is used to explore the radiative cooling-power requirements for long-term antimatter storage. If vacuum-chamber pressures as low as 10^{-18} torr can be reached, and the rest of the large set of assumptions is valid, milligram quantities of solid antimatter could be stored indefinitely at 1.5 K using cooling powers of less than a microwatt. Many of the assumptions made are problematic and need verification, as they could potentially change the results greatly. The system modeled is a sphere of solid anti-parahydrogen at 1.5 K or below levitated in a spherical cryogenic vacuum chamber. The free matter gas in the chamber is assumed to be molecular hydrogen, and sublimation of both matter and antimatter is assumed to be negligible. The antihydrogen is assumed to be in thermal equilibrium, although annihilation-energy deposition is localized and hydrogen's thermal-impulse response time is comparable to the interval between annihilations. A parametric analysis is performed, with system cooling power evaluated over a wide range of pressures and system sizes, as temperature and emissivity are also varied. The cooling-power requirements of storing solid antimatter for extended times may not be an obstacle, if the proper conditions are obtained. However, whether these conditions are indeed possible remains in doubt. Keywords: Solid hydrogen, Fuels, Cryogenic storage, Energy storage, Pions, Annihilation energy deposition, Antiprotons, Annihilation radiation, Theses. (KR)

Table of Contents

Table of Figures

Table of Tables

I Introduction

This project is a study of the cooling-power requirements of a storage system for solid antihydrogen. The approach is analytical, beginning with the derivation of the differential equations governing the system's cooling power. The equations are simplified and solved under quasi-steady-state conditions, and the results incorporated into a computer program that evaluates cooling power requirements as various system parameters are varied.

1 Cryogenic Storage of Antimatter

If a number of technical obstacles can be overcome, the matter-antimatter annihilation reaction may be useful as an energy source for applications requiring compact fuel supplies. For example, no other combination of potential rocket propellants releases more energy per unit mass of fuel. One of the many problems which must be solved if antimatter is to become a practical fuel is how to store antimatter so that it does not react with matter. A very high vacuum and very low temperatures are required to maintain control of the antimatter in storage.

The critical component of antimatter fuel is the antiproton. Unlike the more easily-obtained positron, the antiproton produces energetic charged particles when it annihilates. The momentum of these particles can interact with a magnetic field to accelerate a rocket.[1] Stored antiprotons must be prevented from touching normal matter while in storage, or they will annihilate prematurely. The typical proposed way to maintain control of an aggregate of antiprotons is to combine them with positrons to produce antihydrogen atoms and create a pellet of solid molecular antihydrogen in a vacuum chamber. It may not be possible to solidify a gas without a nucleation site as would be necessary with antimatter; research into this problem is under way.[2] If a solid antihydrogen pellet can be created, the ice ball can be placed in a cryogenic vacuum chamber and levitated electrostatically or magnetically to keep it from touching the chamber walls.

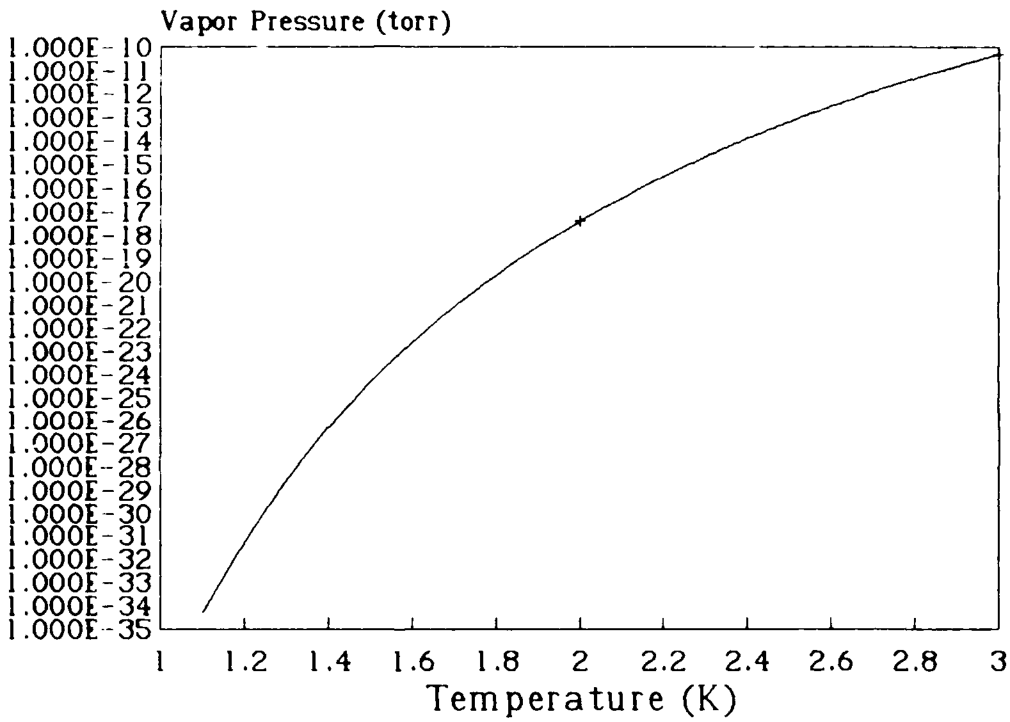

Figure I-1. Vapor Pressure of Solid Parahydrogen

The ice ball must be maintained at a very low temperature in order to keep the antihydrogen from subliming. At temperatures below 1 K the vapor pressure of hydrogen is negligible, so there is no sublimation and the antimatter is effectively contained. Figure I-1 shows an estimate of the behavior of the vapor pressure between 1 and 3 K, derived from a cubic least-squares fit to published calculations of the pressures at 1, 2, 3, and 4 K.[3] As the ice ball's temperature exceeds 1 K, the vapor pressure increases rapidly, prompting increased sublimation rates and eventually allowing significant amounts of antimatter to reach the wall and annihilate. Some of the annihilation radiation is absorbed by the ice ball, raising its temperature and causing further increases in sublimation until the system fails catastrophically.

The very low temperatures and pressures required for this method of storing antimatter may be attainable with current technology. Pomeranchuk cooling systems using ^3He are capable of sustaining 1 microwatt of cooling power at 25 mK.[4] At such low temperatures, the nearly-perfect vacuum required becomes theoretically possible. Sublimation and outgassing of solids are nil, and any gas particles free in the chamber will adhere to the walls on contact. Experiment has shown unpumped vacuum chamber pressures *falling rapidly below* 10^{-14} torr (the minimum measurable) as temperature decreases below 30 K.[5]

2 Scope of Study

The storage system modeled in this study is a spherical cryogenic vacuum chamber containing a spherical antihydrogen ice particle. Several system parameters are varied and their effects on cooling power are numerically computed. The origin of the antihydrogen sphere and its removal from the chamber are not addressed. Temperatures of the antihydrogen ice are allowed to vary from millikelvins to 1.5 K. If the temperature of the antihydrogen rises above 1.5 K, the system is considered to have failed; no analysis is done of the behavior of the system when sublimation becomes significant. The following assumptions are made:

1. The ice ball and the chamber are each characterized by a single temperature. The form of the radiative heat transfer equation used is invalid if temperatures are not uniform. This assumption is correct if the smallest time intervals considered are much larger than the time needed to conduct heat through the chamber wall and the ice ball. The thermal equilibration time of a 0.6-cm hydrogen sphere is on the order of 1 ms.

2. The ice ball is pure anti-parahydrogen. This is the equilibrium condition at the temperatures considered in this study, but the nearness to this condition in a real system will depend on the method used to create the antihydrogen.

3. The chamber wall can be modeled as pure iron for purposes of ionizing-radiation absorption analysis. A typical material for vacuum chambers is type-304 stainless steel, which contains about 35 parts per million of nonferrous elements.[6]

4. The chamber wall is coated on the inside with at least a molecular monolayer of hydrogen, so that its radiative graybody emissivity is the same as that of hydrogen.

5. All of the matter particles free in the vacuum chamber are hydrogen molecules. Thi would be approximately true if the vacuum system had been pumped out sufficiently.

6. Through some leakage or diffusion process, the chamber remains continuously filled with hydrogen gas at constant pressure and at the temperature of the chamber wall.

7. All collisions between hydrogen and antihydrogen molecules result in immediate annihilation of both proton-antiproton pairs and both electron-positron pairs. There is no scattering at the low interaction velocities characteristic of a 1-K environment.

8. Both the ice ball and the chamber wall are "well-behaved" radiative graybodies with diffuse reflection.

II Computation of Cooling Power Requirements

To hold the vacuum-chamber wall at some fixed temperature T_2, any heat energy absorbed by the wall must be removed at the same rate it is deposited. The chamber wall can absorb energy from three sources: heat radiation from the ice ball in the center of the chamber, annihilation radiation from matter-antimatter reactions on the ice ball and on the wall, and adsorption and reverse sublimation of vacuum particles onto the wall. Besides the energy removed from the wall by the cryogenic system, the wall can also lose energy by sublimation and desorption into the chamber.

The extreme low temperature of the system under consideration allows considerable simplification. At such temperatures, there is no sublimation or desorption. Since adsorption of particles still occurs, the vacuum pressure can become arbitrarily low as gas particles adhere to the chamber wall and are not replaced. Since the antihydrogen does not sublime, no antimatter is free to annihilate on the chamber wall. Therefore the central sphere is the only source of annihilation radiation, and this source only lasts as long as it takes for all residual particles to hit either the chamber wall or the sphere. For this study, the system is assumed to contain some hydrogen gas at a constant but very low pressure.

1 System Cooling Power

The required system cooling power can be derived from an energy balance relation for the chamber wall. The chamber wall temperature T_2 is assumed to be constant. Therefore,

$$\frac{dT_2}{dt} = \frac{1}{m_2 c_{v2}} [P_{a2} - P_{s2} + q - P_T] = 0 \tag{1}$$

where m_2 is the mass of the chamber, c_{v2} is the specific heat of the chamber material, P_{a2} is the power deposited in the wall by annihilations on the inner sphere, P_{s2} is power removed by sublimation and desorption from the wall, q is the rate of heat energy transfer from the inner to the outer sphere, and P_T is the total cooling power requirement. Because of the low temperature of the system, there is no sublimation or desorption, however. Solving the above equation for P_T (cancelling out m_2 and c_{v2}) and neglecting the sublimation term,

$$P_T = P_{a2} + q \tag{2}$$

Assuming both surfaces to be gray and reflection to be diffuse, the rate of heat energy transfer from the inner to the outer sphere is[7]

$$q = \frac{\sigma A_1 (T_1^4 - T_2^4)}{\frac{1}{\epsilon_1} + \frac{A_1}{A_2}\left(\frac{1}{\epsilon_2} - 1\right)} \tag{3}$$

$$= \frac{4\pi r_1^2 \sigma (T_1^4 - T_2^4)}{\frac{1}{\epsilon_1} + \frac{r_1^2}{r_2^2}\left(\frac{1}{\epsilon_2} - 1\right)}$$

where σ is the Stefan-Boltzmann constant, T_1, A_1, r_1, and ϵ_1 are the temperature, surface area, radius, and emissivity of the ice ball, and the corresponding quantities subscripted with a 2 refer to the chamber wall. Strictly speaking, the substances' emissivities depend on temperature, but over the narrow temperature range under consideration here it is justifiable to assume they are constant.

The power deposited in the wall by annihilations in the central sphere is given by

$$P_{a2} = (E_{a1} + E_{a2}) R_{a1} \tag{4}$$

where R_{a1} is the annihilation rate in the central sphere, E_{a1} is the energy deposited in the central sphere per annihilation in the sphere, and E_{a2} is the energy deposited in the wall per annihilation in the sphere.

The annihilation rate in the inner sphere is simply the collision rate for the vacuum gas with the surface of the inner sphere, derivable from the kinetic theory of gases:[8]

$$\begin{aligned} R_{a1} &= 4\pi r_1^2 \frac{1}{4} n_v v_m \\ &= 4\pi r_1^2 \frac{1}{4}\left(\frac{P_v}{kT_v}\right)\left(2\sqrt{\frac{2kT_v}{\pi m_v}}\right) \\ &= \frac{4\pi r_1^2 P_v}{\sqrt{2\pi m_v k T_v}}. \end{aligned} \tag{5}$$

Here n_V is the vacuum number density, v_m is the mean gas particle velocity, P_V is the vacuum chamber pressure, m_V is the mass of a gas molecule, T_V is the gas temperature, and k is Boltzmann's constant. At a fixed chamber pressure, there is thus an inverse dependence of the collision rate on gas temperature, devolving from the ideal-gas law relating temperature, pressure, and number density.

2 Annihilation Energy Deposition

The mutual annihilation of a hydrogen atom and an antihydrogen atom liberates the rest mass energy of two protons and two electrons, or 1877 MeV. Since the free particles in the vacuum chamber are assumed to be diatomic hydrogen molecules, each collision yields 3755 MeV. The energy from a proton-antiproton annihilation appears in the form of charged and neutral pions. Forward[9] reports that each proton-antiproton annihilation releases its energy on the average in the form of 3.0 charged pions and 1.5 neutral pions, (as well as negligible amounts of other products: 0.08 kaons and 0.02 prompt gamma rays per annihilation). The neutral pions decay immediately to high-energy gamma photon pairs. The energy from an electron-positron annihilation appears as two (or rarely in solids, three) gamma photons. The energy deposition modes to be considered are thus charged pions, pion-decay gammas, and annihilation gammas.

Energy Deposition in the Antihydrogen Sphere

Charged Pions

Figure II-1 shows the energy spectrum of the charged pions from a low-energy proton-antiproton collision. Gaines[10] divides the pion spectrum into approximately 70 energy groups and finds the average stopping power of solid hydrogen for a single charged pion from this energy spectrum:

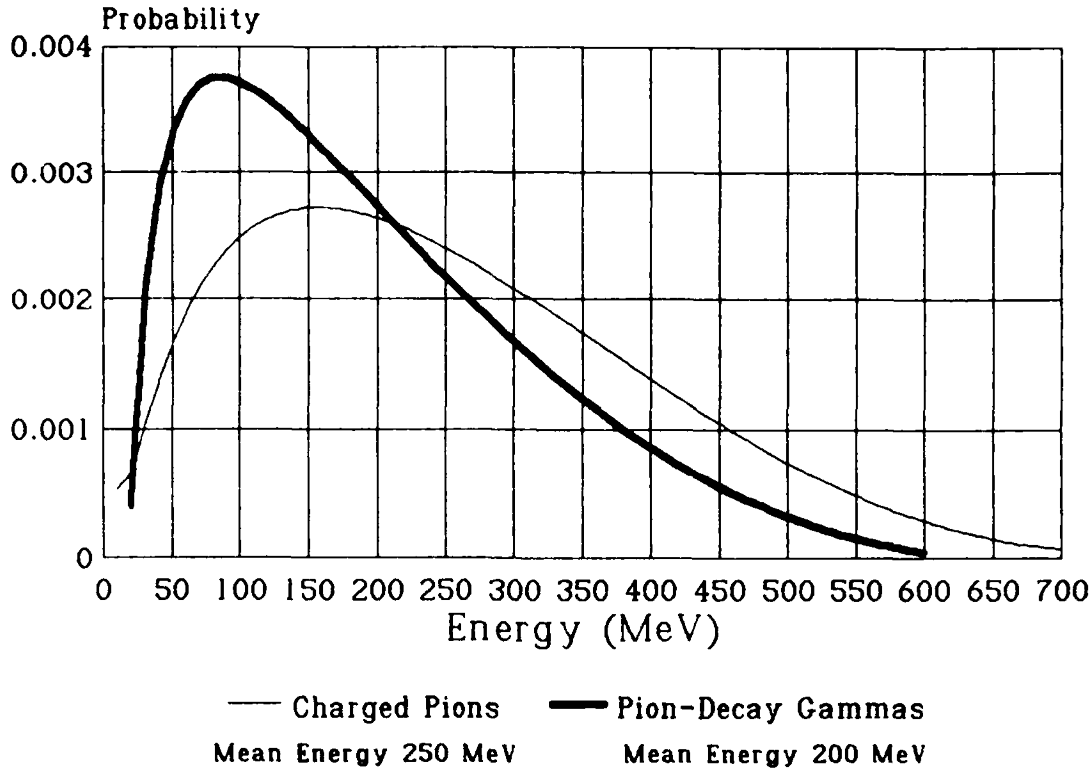

Figure II-1. Charged-Pion and Gamma Energy Spectra

$$\left\langle \frac{\mathbf{d}E}{\mathbf{d}x} \right\rangle_{\pi 1} = 0.437 \quad \text{MeV/cm} \tag{6}$$

$$= 7.00 \cdot 10^{-12} \quad \text{J/m}.$$

This formulation assumes the pion's energy, and hence the stopping power, remains nearly constant as the particle traverses the hydrogen. This can be seen to be valid for the pion energies (on the order of hundreds of MeV) and hydrogen path lengths (on the order of millimeters) under consideration here.

Given the average energy deposition per pion, the mean energy deposited per molecular annihilation can be calculated. Each molecular annihilation produces an average of six charged pions, three from each proton-antiproton pair. Since the reaction products are emitted isotropically, only half the total number, or three per molecular annihilation, pass through the hydrogen sphere. Thus the energy deposited in the hydrogen by a single molecular collision is

$$E_{\pi 1} = 3.00 \cdot (7.00 \cdot 10^{-12}\,\mathrm{J/m}) \langle x \rangle \tag{7}$$

$$= (2.10 \cdot 10^{-11}\,\mathrm{J/m}) \cdot \frac{d}{\pi}$$

where d is the diameter of the sphere and $\langle x \rangle = d/\pi$ is a mean chord length through the sphere. This analysis differs from Gaines' in using $\langle x \rangle$ instead of the full diameter, and in assuming molecular rather than single-proton collisions.

Gamma Rays from Neutral-Pion Decay

The neutral pions decay to pairs of gamma rays after a mean lifetime of just 9.0×10^{-17} seconds, before they can deposit any significant amount of energy in the system. The gamma rays resulting from the pion decay, however, do deposit energy. The energy spectrum of the pion-decay gammas is also given in Figure II-1. Gaines uses the decay-gamma spectrum in Figure II-1 to compute an average linear gamma attenuation factor of 0.198 MeV/cm. Thus for a molecular annihilation, three neutral pions will be produced which will decay to six gammas, three of which will penetrate the hydrogen and deposit

$$E_{\gamma\pi 1} = 3.00 \cdot (0.198\,\mathrm{MeV/cm}) \cdot \langle x \rangle \tag{8}$$

$$= (9.52 \cdot 10^{-12}\,\mathrm{J/m}) \cdot \frac{d}{\pi}.$$

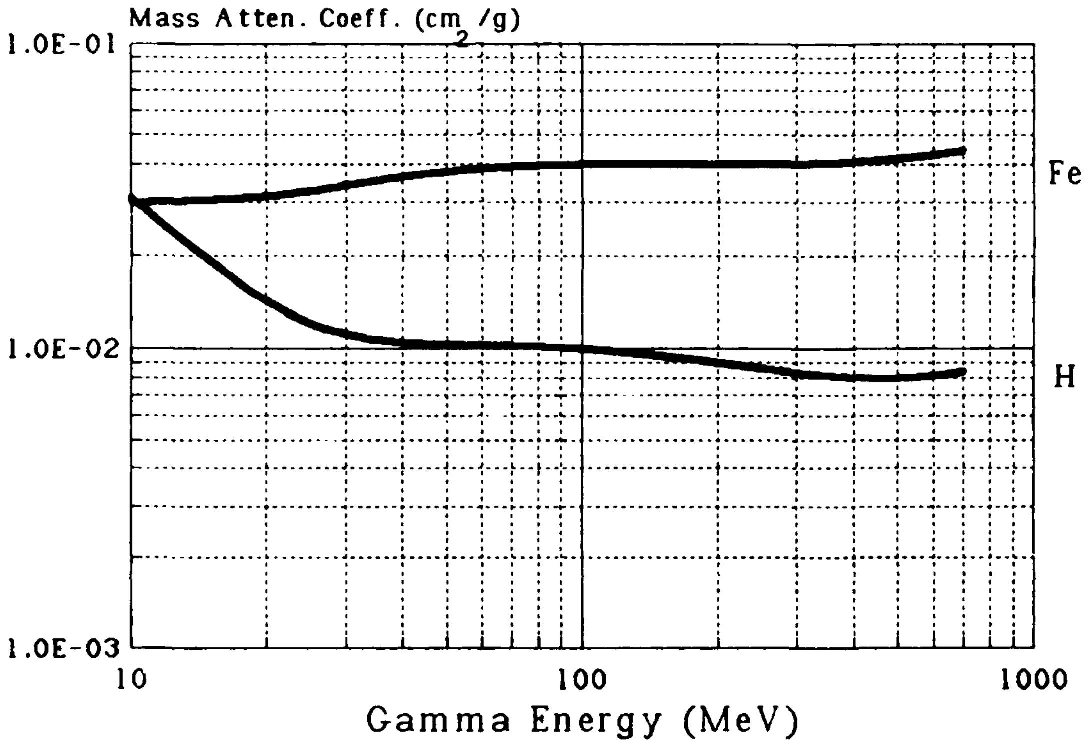

Figure II-2. Gamma Attenuation Coefficients in Iron and Hydrogen

The gamma-ray portion of Gaines' analysis is for single-proton collisions with the gammas traversing the entire diameter of the sphere as before, and it erroneously stipulates that each neutral pion decays into one gamma, not two. Gaines' linear model of gamma energy deposition is valid because the size of the hydrogen ball is very small compared to the interaction lengths of these high-energy gammas, as shown in Figure II-2. For example, the interaction length of a comparatively less-penetrating 10-MeV gamma is

$$\lambda = \left(\frac{\mu}{\rho}\rho\right)^{-1} \tag{9}$$

$$= (0.21\,\mathrm{cm}^2/\mathrm{g} \cdot 0.0893\,\mathrm{g/cm}^3)^{-1}$$

$$= \frac{1}{0.018\,\mathrm{cm}}$$

$$= 53\,\mathrm{cm}$$

where $\rho = 0.0893$ $\mathrm{g/cm}^3$ is the density of solid hydrogen at zero pressure.

Gamma Rays from Electron-Positron Annihilation

In solids, the annihilation of electrons and positrons almost always produces a single pair of 511-keV gamma photons. The energy deposited by such photons in a mean chord $\langle x \rangle$ of a solid-hydrogen sphere is

$$E_{\gamma e1} = (511\,\mathrm{keV}) \frac{\mu_{en}/\rho}{\mu_t/\rho}(1 - e^{-(\mu_t/\rho)(\rho)\langle x \rangle}) \tag{10}$$

$$= (8.19 \cdot 10^{-14}\,\mathrm{J}) \frac{0.060}{0.12}(1 - e^{-(0.12\,\mathrm{cm}^2/\mathrm{g})(0.0893\,\mathrm{g/cm}^3)(d/\pi)})$$

$$= (4.09 \cdot 10^{-14}\,\mathrm{J})(1 - e^{-(0.0107\,\mathrm{cm}^{-1})(d/\pi)})$$

where the factor μ_{en}/μ_t accounts for non-local energy deposition, and the total and energy-deposition cross sections are those of molecular hydrogen.[11] For reasonably large values of d, the energy deposition from electron-positron annihilation is sufficiently small compared to the energy deposition from charged pions to be neglected. For example, a small ice particle of 2.0 ng mass, with a diameter of 0.0036 cm, will absorb 1.5×10^{-20} J from annihilation photons and 9.7×10^{-14} J from charged pions.

Total Annihilation Energy Deposited in Antihydrogen

The contributions from charged and neutral pions can now be summed (neglecting the annihilation gammas), giving

$$E_{a1} = E_{\pi 1} + E_{\gamma\pi 1} \tag{11}$$

$$= (2.10 \cdot 10^{-11} \mathrm{J/m} + 9.5 \cdot 10^{-12} \mathrm{J/m}) \frac{d}{\pi}$$

$$= (3.05 \cdot 10^{-11} \mathrm{J/m}) \frac{d}{\pi}.$$

as the expression for the total annihilation energy deposited in the antihydrogen sphere per molecular collision.

Energy Deposition in the Chamber Wall

Gaines does not extend his analysis of annihilation-energy deposition in hydrogen to the deposition of this energy in a steel wall. The same techniques are applicable, but since the wall thickness is not as much less than the interaction lengths for pions and gammas, more accurate alternative methods are used for this study. Annihilation energy strikes the wall in the form of charged pions and pion-decay gammas from annihilations on the antihydrogen sphere. As in the antihydrogen, gammas from electron-positron annihilation are not important sources of energy. The total annihilation energy deposited in the wall is

$$E_{\alpha 2} = E_{\pi 2} + E_{\gamma 2} \tag{12}$$

where the energy deposited by charged pions is determined from tables of pion ranges in iron, given an assumed thickness x of the chamber wall.

Charged Pions

In a residual-range calculation, the energy deposited is determined by finding the range of the pion in the material at the incident energy and subtracting the thickness of the material to find the pion's remaining range in the material. The pion energy associated with this range is found from the range table and stipulated to be the pirn's energy upon exiting the wall. The energy deposited is just the difference between the entering and exiting pion energies. This process is repeated over many pion-energy bands, and the fractional results are summed to reach the total pion energy deposited.

Gamma Rays from Neutral-Pion Decay

The energy deposited by pion-decay gammas is also calculated by summing the contribution of many energy bands, as

$$E_{\gamma} = \sum_{i} f_i E_i \frac{\mu_{en}}{\mu_i} \left(1 - e^{-(\mu_i/\rho)(\rho)x} \right) \tag{13}$$

where f_i is the fraction of the spectrum modeled as having energy E_i. Here x represents the thickness of iron traversed by the radiation, which is approximately the thickness of the chamber wall since the radiation originates near the center of a spherical chamber. The factor μ_{en}/μ_t is to account for a fraction of the energy released from a photon-matter interaction not being deposited locally.

This device, the energy-transfer ratio, is not useful at the high photon energies (greater than 10 MeV) under consideration here. At such energies, pair production is the most likely interaction mode. Although only a fraction of the incident photons will interact with the target matter along a given linear path length, those causing pair productions may transfer nearly all of their energy to the resulting energetic electron-positron pair. The energetic electron thus produced may deposit all its energy in the material or may escape, carrying off some energy. The positron also may escape, and if it is stopped, it will be annihilated and produce 511-keV photons, which may also escape. Both the electron and the positron emit Bremsstrahlung radiation which may also escape. The fraction of interaction energy which remains in the system is thus very sensitive to the materials and geometry of the wall. As a worst-case simplification, the ratio μ_{en}/μ_t is assumed to be unity in this study.

3 Temperature of the Central Sphere

The inner sphere's temperature is governed by radiative exchange with the chamber wall, and by the annihilation-energy deposition rate. If the ice ball's mass m_1 is assumed to be constant, the rate of change of the ice ball's temperature is

$$\frac{dT_1}{dt} = \frac{1}{m_1 c_{v1}}(P_{a1} - q) \tag{14}$$

where P_{a1} represents the annihilation-energy deposition rate on the inner sphere. The specific heat c_{v1} can be calculated from a simplified expression of the Debye formula[12]

$$c_{v1} = \frac{12\pi^4 R}{5M_H}\left(\frac{T}{\theta_D}\right)^3 \tag{15}$$

since the temperatures under consideration are low compared to hydrogen's Debye temperature $\theta_D = 120.3\text{K}$. The factors R and M_H in the Debye equation represent the gas constant and the molecular weight of hydrogen.

4 Antihydrogen Sublimation

Equilibrium Sublimation Rate

For this study, a temperature range is chosen within which there is effectively no sublimation of solid parahydrogen. The sublimation rate at a given temperature can be estimated in two ways, which together provide an upper and lower bound on the sublimation rate.

An upper bound can be placed on the sublimation rate if one assumes that the lattice is vibrating at its maximum frequency, that associated with the Debye temperature. In this case, the Arrhenius relation gives the resulting sublimation rate as[13]

$$R_A = \nu_m n_s e^{\Delta E_s / kT_1} \tag{16}$$

$$= \left(\frac{k\theta_D}{h}\right)\left(4\pi \frac{r_1^2}{\lambda_s^2}\right) e^{kT_s/kT_1}$$

$$= \left[\frac{4k\pi}{h} \frac{120.3\text{K}}{(3.7 \cdot 10^{-10}\text{m})^2}\right] r_1^2 e^{(-89.8\text{K})/T}$$

where ν_m is the vibration frequency, n_S is the number of molecules on the surface, ΔE_s is the enthalpy of sublimation, h is Planck's constant, and λ_s is the intermolecular spacing. At a given temperature, the sublimation rate can be no higher than that given by this expression, since the lattice vibrations can be no faster than ν_m.

The sublimation rate can be bounded below by reasoning from a hypothetical case where the hydrogen or antihydrogen is in equilibrium with its vapor. Under such conditions, the rate of sublimation must equal the rate of collision of vapor particles with the surface. The sublimation rate will therefore be

$$R_e = \frac{4\pi r_1^2 P_V}{\sqrt{2\pi m_H k T_1}} \tag{17}$$

where P_V is the vapor pressure from Figure I-1 and m_H is the mass of a hydrogen molecule. The solid in vacuum should not sublime any more slowly than it does in equilibrium.

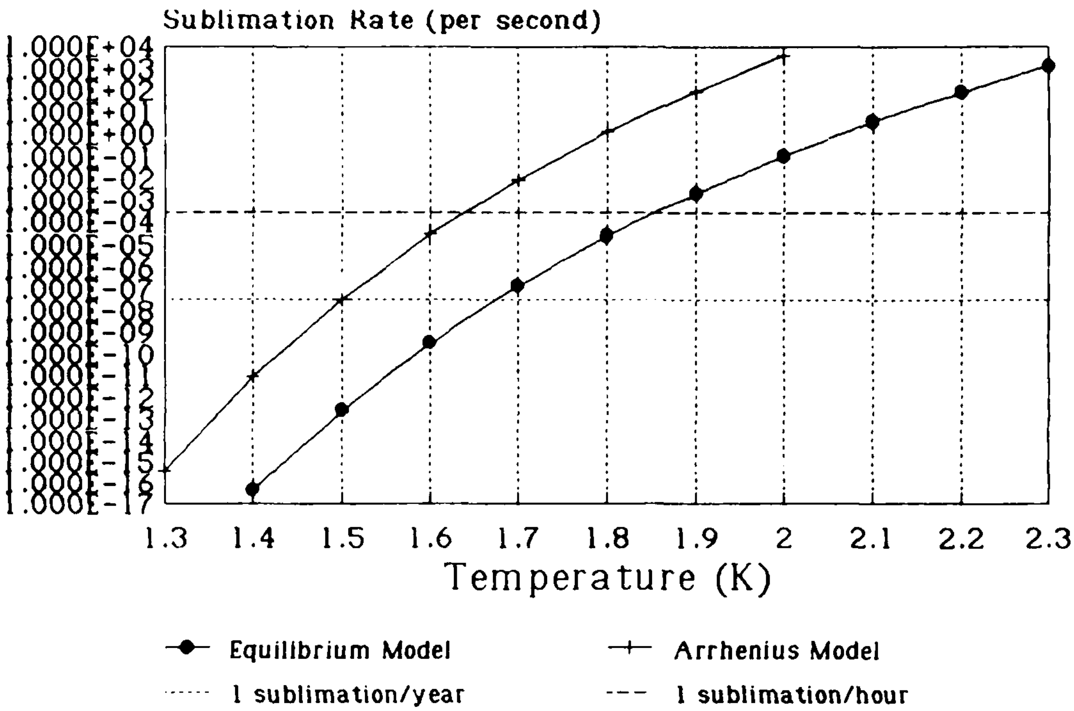

Figure II-3. Sublimation Rates in a 1-mg Solid-Hydrogen Sphere

Figure II-3 shows the two estimates of the sublimation rate. Based on these calculations, it seems credible to consider the sublimation rate to be effectively zero at temperatures as high as 1.5 K. This, however, ignores the possibility of localized sublimation caused by the deposition of annihilation energy.

Local Sublimation

Local energy deposition by annihilation radiation may be sufficient to cause sublimation. This possibility can be examined using the stopping power and linear attenuation factor computed by Gaines. The energy required to sublime a single hydrogen molecule is[14]

$$\Delta E_s = kT_s \tag{18}$$

$$= (1.38 \cdot 10^{-23} \mathrm{J/K})(89.8\mathrm{K})$$

$$= 1.24 \cdot 10^{-21} \mathrm{J}$$

$$= 7.74 \cdot 10^{-3} \mathrm{eV}.$$

If a single charged pion deposits 0.437 MeV per centimeter of hydrogen traversed, and the intermolecular spacing is 3.7 angstroms, then each molecule along the pion's path absorbs

$$\Delta E_\pi = \left\langle \frac{\mathrm{d}E}{\mathrm{d}x} \right\rangle_\pi \lambda_s \tag{19}$$

$$= (4.37 \cdot 10^{5} \mathrm{eV/cm})(3.7 \cdot 10^{-8} \mathrm{cm})$$

$$= 1.62 \cdot 10^{-2} \mathrm{eV}$$

$$= 2.09 \cdot \Delta E_s.$$

Thus if all of the absorbed energy went into heating a single string of molecules, it would take only one pion track to cause considerable sublimation.

In fact, however, the energy is not deposited along a one-dimensional string. The gamma rays from neutral-pion decay, which have approximately half the charged pions' linear energy transfer rate, deposit their energy throughout the solid. A charged pion deposits its energy in a cylindrical annulus of dimensions determined by the minimum and maximum possible impact parameters for electromagnetic interaction for the energy of the pion.[15] For a 250-MeV pion with

$$\gamma = 1 + \frac{T}{m_0 c^2} \tag{20}$$

$$= 1 + \frac{250\,\mathrm{MeV}}{139.6\,\mathrm{MeV}}$$

$$= 2.79$$

the minimum impact parameter is effectively zero:

$$b_{min} = \frac{\hbar}{\gamma m_e v} \tag{21}$$

$$= \frac{\hbar c}{\gamma m_e c^2 \sqrt{1 - \gamma^{-2}}}$$

$$= \frac{1.973 \cdot 10^{-13}\,\mathrm{MeV \cdot m}}{(2.79)(0.511\,\mathrm{MeV})\sqrt{1 - 2.79^{-2}}}$$

$$= 1.48 \cdot 10^{-13}\,\mathrm{m}.$$

The maximum impact parameter is

$$b_{max} = \frac{\hbar v \gamma}{I} \tag{22}$$

$$= \frac{\hbar}{I} \gamma c \sqrt{1 - \gamma^{-2}}$$

$$= \frac{(6.582 \cdot 10^{-16} eV \cdot s)(2.79)(2.998 \cdot 10^{8} m/s)}{18.2 eV} \sqrt{1 - 2.79^{-2}}$$

$$= 2.82 \cdot 10^{-8} m$$

where I = 18.2 eV is the mean ionization potential of molecular hydrogen.[16] Considering the energy-deposition region as a cylinder of radius b_{max}, the mean energy deposited per molecule is

$$\overline{\Delta E_{\pi}} = (1.62 \cdot 10^{-2} eV) \frac{(3.7 \cdot 10^{-10} m)^2}{4\pi (2.82 \cdot 10^{-8} m)^2} \tag{23}$$

$$= 2.21 \cdot 10^{-7} eV.$$

Averaged over the entire charged-pion spectrum, the mean energy deposition is 4.71 x 10^{-7} eV per molecule, still well below the energy needed for sublimation. However, since energy deposition is not constant throughout the cylinder, but rather varies as $1/r^2$, this is not necessarily a conclusive demonstration that annihilation radiation will not stimulate local sublimation of the antihydrogen.

5 Heat Transport in Solid Hydrogen

The speed with which the added heat from a localized energy deposition travels bears on the validity of a single-temperature model of the ice ball. In order for the model to be valid, the time required for the heat impulse to travel across the ball must be small compared to the time interval between energy depositions.

The ice ball's response to a heat impulse is given by the Green's function for the heat equation:[17]

$$G(r,t) = (4\pi\alpha t)^{-n/2} e^{-r^2/4\alpha t} \tag{24}$$

where α is the thermal diffusivity of the material and n is the number of dimensions. If the annihilation impulse is deposited along a narrow track, the system approximates a two-dimensional geometry, so that

$$G(r,t) = \left(\frac{4\pi k_1 t}{\rho_1 c_{v1}}\right)^{-n/2} e^{-r^2\rho_1 c_{v1}/4k_1 t} \tag{25}$$

$$= \left(\frac{4\pi(5M_H\theta_D^3)t}{(12\pi^4 RT^3)\rho_1}\right)^{-n/2} e^{-r^2\rho_1(12\pi^4 RT^3)/4(5M_H\theta_D^3)t}$$

where the thermal conductivity k_1 = 2.5 W/m/K at 1.5 K.[18] Figure II-4 is a graph of the Green's function at T = 1.5 K and r = 0.6 and 1.2 cm, the radius and diameter of a 10-mg hydrogen sphere. The figure shows the impulse response peaking at times near 1 microsecond after the impulse, and decaying to 10% of its peak value after less than 100 microseconds. For a 10-mg sphere at 1.5 K, a collision rate of 1 per 7 x 10^{-5} seconds corresponds to a vacuum pressure of 2.0 x 10^{-17} Pa, or 1.6 x 10^{-19} torr.

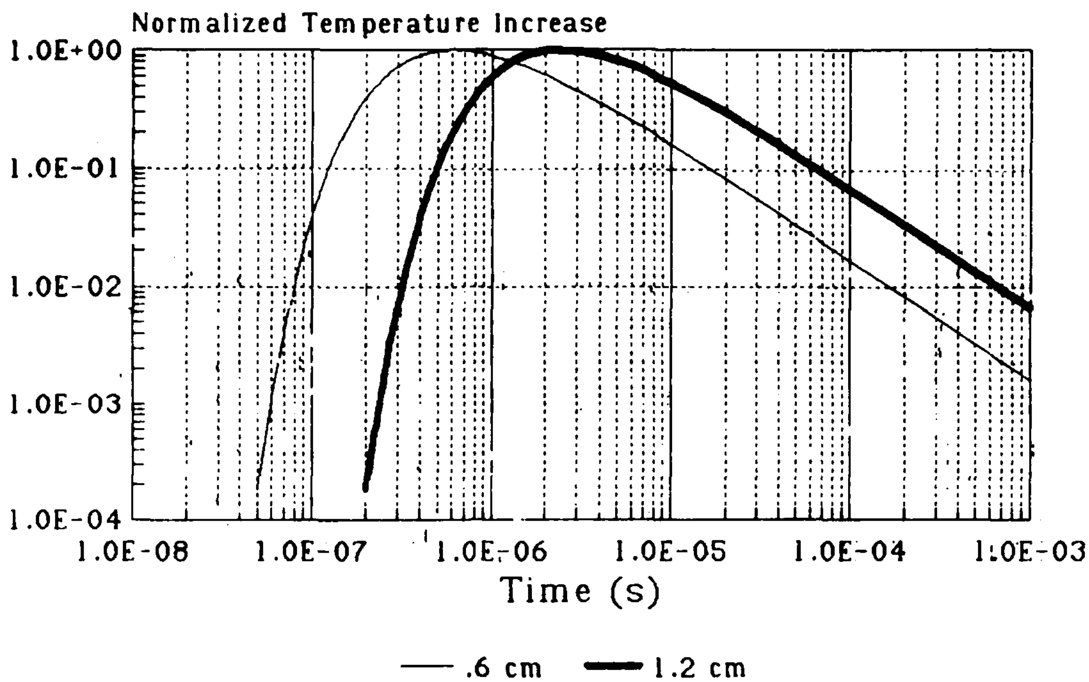

Figure II-4. Heat Impulse Response for .6 and 1.2 cm Thicknesses of Solid Hydrogen.

III Simulation of a Cryogenic Antihydrogen Storage System

The analysis given in the previous section provides the basis for a computer program to determine the cooling-power requirements of a simple antihydrogen storage system. In this program, several system parameters are varied to determine their effect on cooling power: the temperatures of the antimatter ball and the chamber wall, the vacuum-chamber pressure, the chamber radius, and the mass of the antimatter ball, and the emissivity of solid hydrogen.

Some needed numbers are not available, including the graybody emissivity of solid hydrogen and the precise spectra of the proton-antiproton annihilation products. Apparently solid hydrogen's emissivity is still unknown. In his analysis, Gaines assumes an emissivity of 0.5 without justification. In this program, the emissivity is simply varied as a parameter. At this writing, precise figures have not yet been obtained on the energy spectra of proton-antiproton annihilation products. These data exist, but do not seem to be published in numerical form. As a rough estimate, an exponential fit was done to a number of values read from the spectra in Gaines' report. On normalizing this fit, it becomes apparent that Gaines' graphs, which he obtained by digitizing an unscaled graph in Forward's report, give probabilities which are too high by a factor of ten (though Gaines' results based on the spectra are correct). The fits used for this study are correctly normalized.

1 Description of the Implementation

The program uses a finite-difference method, describing the system in terms of incremental energy releases over short time intervals. The energy incident on the chamber wall is evaluated over a brief time increment and divided by the time to determine the rate of energy influx and thence the cooling power required during that time. The chosen time increment is 1 ms, the time required for a heat impulse to subside to 1% of its peak value at a distance of 1.2 cm from the event. As will be shown in the next section, the regime of operation in this study was effectively steady-state: at the collision rates considered, the ice ball temperature is constant over any reasonable system lifetime. Therefore, for each set of parameters, the results after the first iteration are considered to hold continuously. The program can be divided in two parts: a preliminary portion where the environment is set up, and a working portion in which a single parameter is varied.

Preliminary Setup

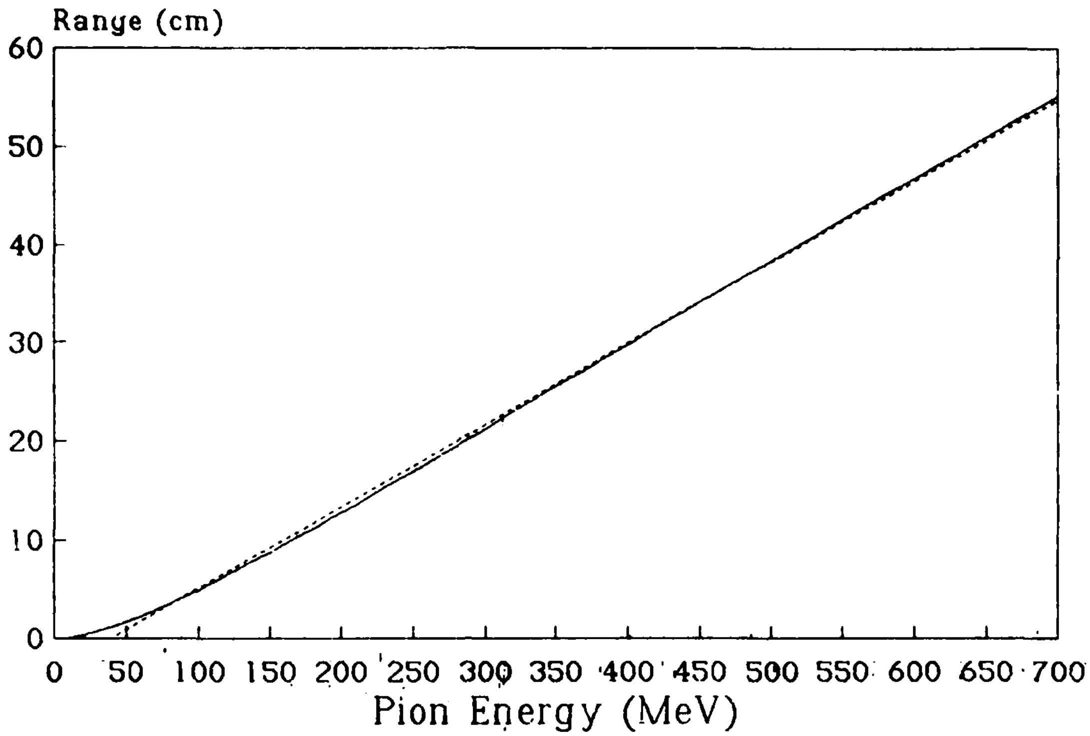

Figure III-1. Pion Ranges in Iron.

Before beginning to vary the chosen parameter, various environmental quantities must be calculated. The ice ball's radius is calculated from its mass, and then used in equations (5) and (11) above to determine the annihilation rate R_{a1} and the energy deposition per annihilation E_{a1}. The product of R_{a1} and E_{a1} is the annihilation power to the ice ball $Pa1$. The charged-pion energy deposition to the chamber wall is computed by the residual-range method with the pion range function approximating published range data[19] with the linear least-squares fit RANGE = (0.082757 cm/MeV)x - (3.19505 cm), as shown in Figure III-1. Gamma rays are attenuated exponentially, using the cross section curve shown in Figure II-2:

$$\frac{\mu_t}{\rho}=\frac{-5.4549037}{(\ln E)^2}+\frac{1.9320344}{\ln E}+\frac{17.519744}{E^2}+\frac{1.9017611}{E}$$
$$+(2.851937\cdot 10^{-5})E-0.1458238 \qquad (26)$$

where E is in MeV and μ_t/ρ is in cm^2/g. Gaines' figures, appropriately modified as discussed in the previous chapter, are used to evaluate annihilation energy incident on the antimatter sphere. In the absence of numerical data on pion and gamma energies, the spectra were approximated as

$$f(E)=Ae^{BE}+Ce^{DE}+F(\ln E)^2+G\ln E+HE^2+IE+J \qquad (27)$$

where E is in MeV and the coefficient values are given in Table III-1.

Table III-1. Exponential Fit Coefficients for Pion and Gamma Spectra

Coefficient	Pion Spectrum	Gamma Spectrum
A	-0.1238	-0.1411
B	9.9572×10^{-7}	1.08615×10^{-6}
C	7.071×10^{-2}	5.578×10^{-2}
D	-1.0187×10^{-6}	-1.0481×10^{-6}
F	1.018×10^{-3}	-1.632×10^{-3}
G	-6.106×10^{-3}	1.443×10^{-2}
H	2.809×10^{-8}	7.985×10^{-9}
I	-5.666×10^{-5}	-9.453×10^{-8}
J	7.867×10^{-2}	5.709×10^{-2}

Variation of Parameters

For each value of the parameter under study, a single iteration of the time-dependent model is run. This entails computing the radiant power q using equation (3), then adding it to the annihilation power P_{a2} to find the total cooling power P_T as shown in equation (2). The temperature increase rate dT_1/dt is computed from equation (14), with the heat capacity c_{v1} given by equation (15). If further iterations were to be done, the temperature would then be increased by $(dT_1/dt)dt$, the time incremented by dt, and the process begun again with the new temperature T_1. At the low annihilation rates considered, however, dT_1/dt is approximately zero.

2 Summary of Relevant Quantities

The quantities dealt with can be categorized according to whether they are given or assumed, calculated (derived), or are variable parameters. A summary of the relevant quantities appears below.

Known Quantities

The Debye temperature of solid hydrogen $\theta_D = 120.3K$).[20]

Hydrogen and iron cross sections for pions and gammas.

Annihilation-product energy spectra.

Calculated Quantities

Specific heat of solid hydrogen as a function of temperature (c_{v1}).

Antihydrogen temperature (T_1) as a function of time.

Radius of the antihydrogen ball (m_1)

Annihilation energy deposition rate in antihydrogen (P_{a1}).

Annihilation energy deposition rate in the wall (P_{a2}).

Parameters to be Varied

A total of seven parameters are varied one at a time. When a parameter is not being varied, it is given a baseline value selected to place the system in a near steady-state condition. The parameters and their baseline values are:

1. Constant pressure of vacuum (P_V). This parameter is varied from 10^{-40} torr to 1 torr, with a value of 10^{-19} torr in the baseline case.

2. Mass of the antihydrogen ice ball (r_1). This parameter is varied between 1 ng and 1 kg, with 10 mg as the baseline case.

3. Radius of the vacuum chamber (r_2). This parameter is varied from 1.1 to 100 times the ice ball radius, and has a baseline value of 0.1 m.

4. Constant temperature of the chamber wall (T_2). This parameter is varied from 0.01 K to 1.50 K. Its baseline value is 1.00 K.

5. Initial temperature of the ice ball (T_{01}). This temperature also runs from 0.01 K to 1.50 K, but its baseline value is 1.50 K.

6. Emissivity of solid hydrogen (ϵ_1). This quantity has apparently not been measured, so it is varied as a parameter between 0.001 and 1.000, with a baseline value of 0.050.

7. Thickness of the chamber wall. A baseline value of 1.0 cm is used, but this parameter is varied between 0.5 cm and 3.0 cm to allow for different vacuum-chamber designs.

IV Results of Simulation

1 Effect of Chamber Pressure

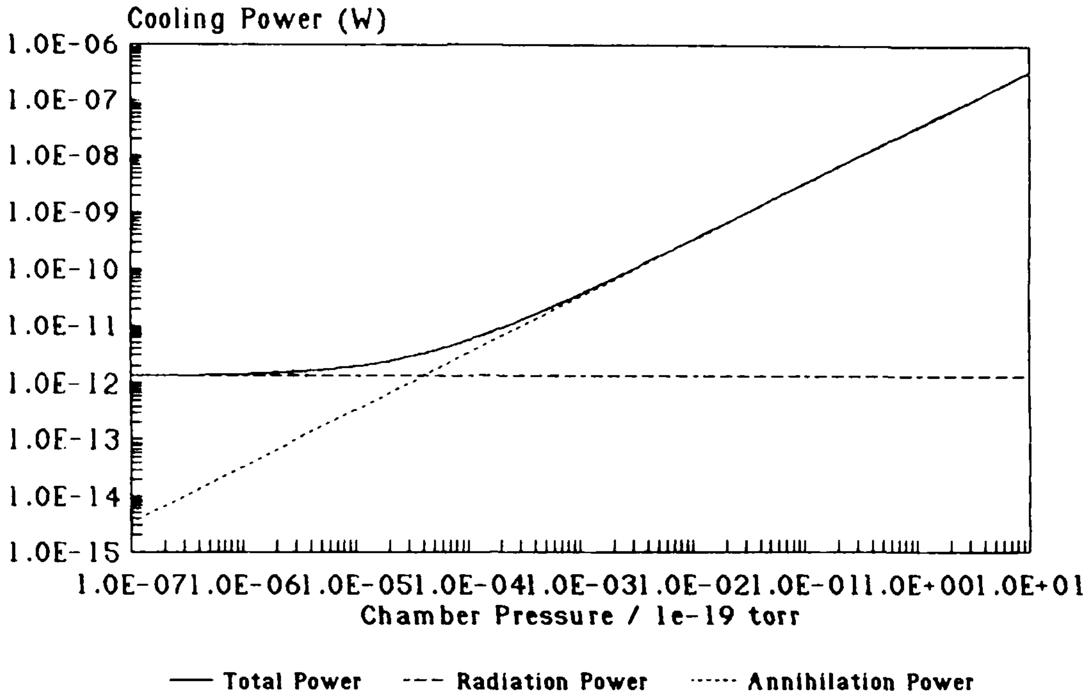

Figure IV-1a. Cooling Power Requirement at Various Chamber Pressures

The pressure to which the vacuum chamber can be evacuated is the key parameter of the seven investigated here. Figure IV-1a shows the effect of chamber pressure (in units of 10^{-19} torr) on system cooling power. The figure shows the radiative and annihilation components of the cooling power, demonstrating that operation above about 10^{-23} torr is dominated by annihilation, and operation below about 10^{-24} torr is dominated by thermal radiation. The cooling power does not approach 1 microwatt until pressure is above 10^{-18} torr. The following variations of the other parameters were run at four chamber pressures. In addition to the baseline case of 10^{-19} torr, 10^{-14}, 10^{-16}, and 10^{-22} torr were examined.

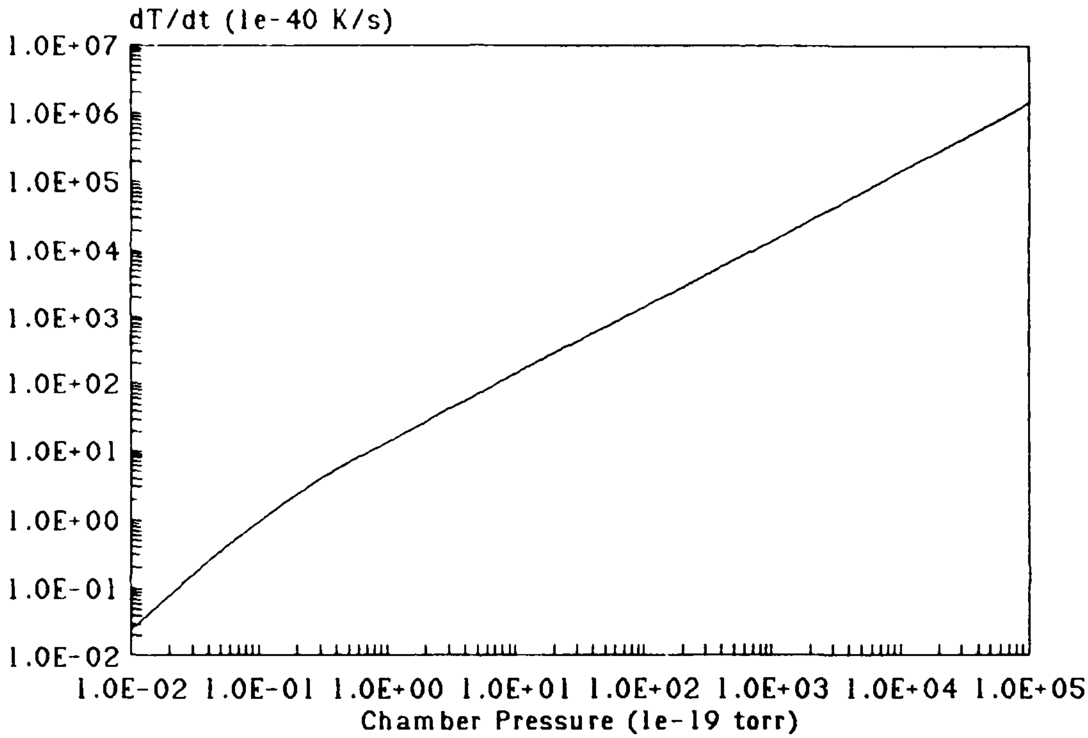

Figure IV-1b. Temperature Increase Rate at Various Chamber Pressures

Another factor of interest is the temperature increase rate of the ice ball, dT_I/dT. Figure IV-1b shows that the system can indeed be considered steady-state at the chamber pressures under consideration here.

2 Effect of Antihydrogen Mass

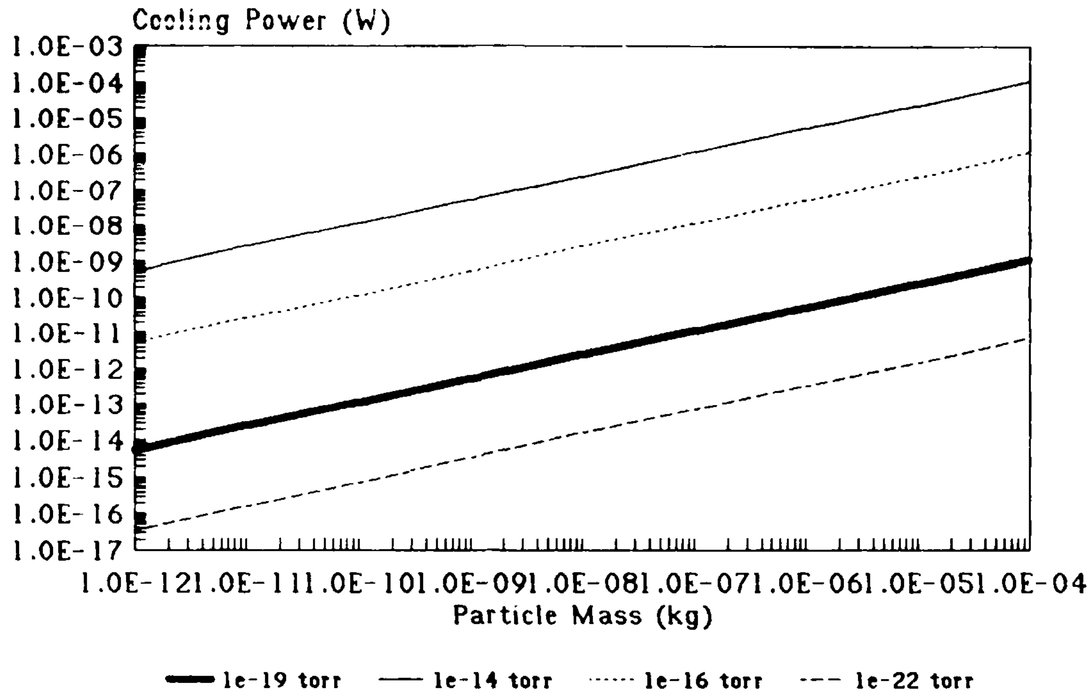

Figure IV-2. Cooling Power Requirement for Various Antihydrogen Masses

Figure IV-2 shows the effects of pressure and ice-ball mass on the system cooling power. As one might expect, the mass of antimatter contained has a significant influence on system cooling power. There is no qualitative difference in the effect of mass at high and low pressures.

3 Effect of Chamber Radius

The radius of the vacuum chamber effects the cooling power only when the chamber radius is very close to the ice ball radius and the system is operating at a pressure such that the radiative component of the cooling power is significant. This effect can be seen in the 10^{-22}-torr line in Figure IV-3.

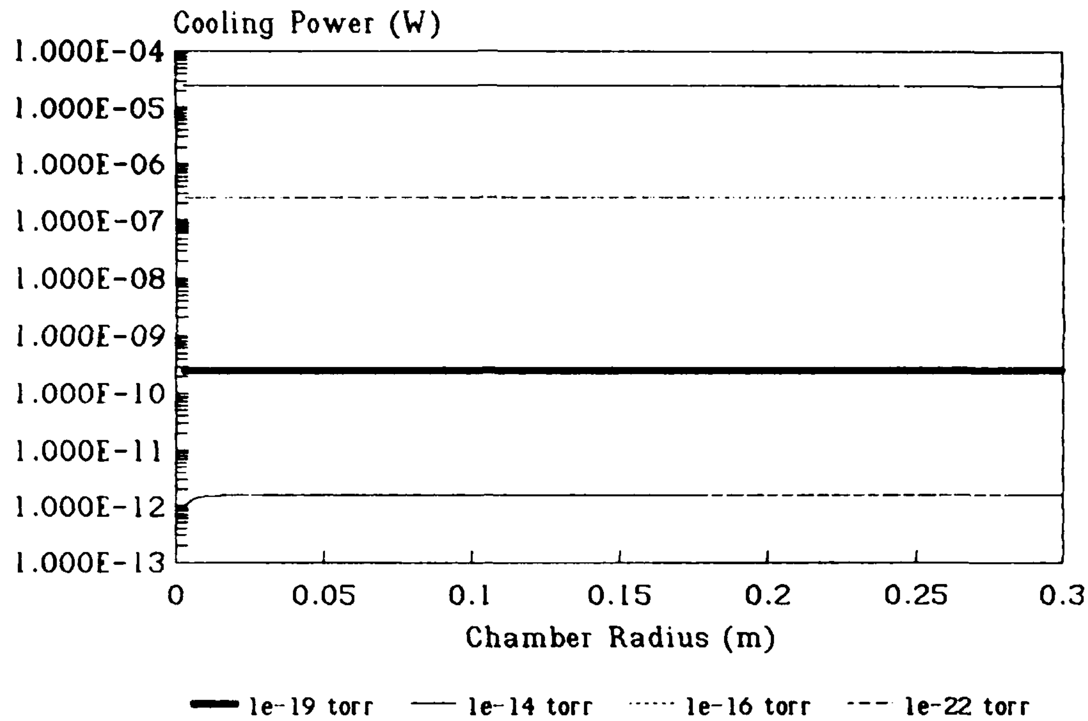

Figure IV-3. Cooling Power Requirement for Various chamber Radii

4 Effect of Wall Temperature

Figure IV-4 shows that with the ice ball fixed at 1.5 K, varying the wall temperature produces little change in cooling power. The effect is somewhat greater if the pressure places the system in a radiation-dominated power regime.

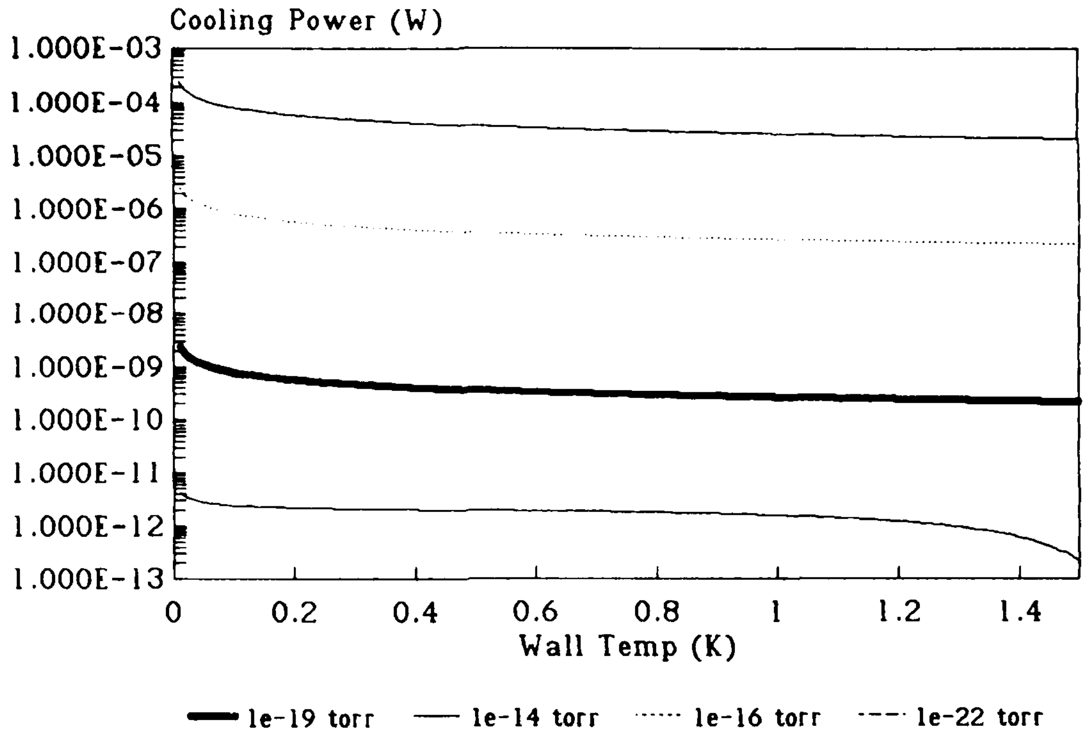

Figure IV-4. Cooling Power Requirement at Various Wall Temperatures

5 <u>Effect of Antihydrogen Temperature</u>

The ice ball's temperature is a significant factor only at low pressures, when radiation dominates annihilation power. Otherwise, it has no effect on the cooling power, as shown in Figure IV-5.

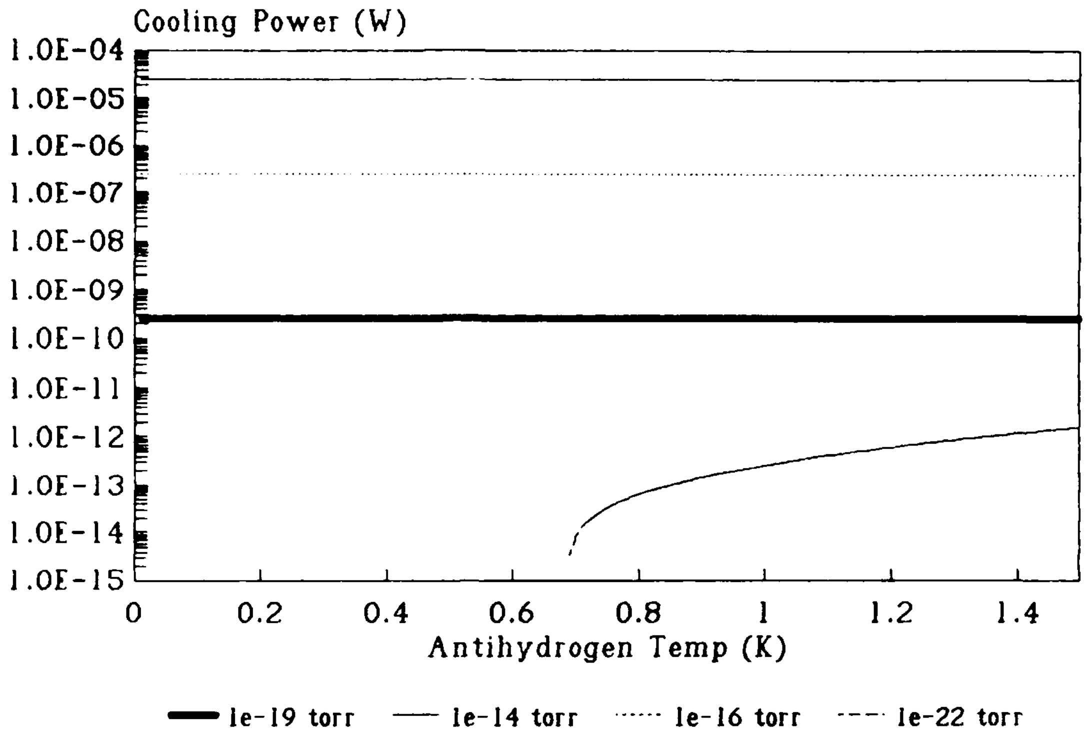

Figure IV-5. Cooling Power at Various Antihydrogen Temperatures

6 Effect of Hydrogen Emissivity

Emissivity is another factor that is significant only at low pressures, as shown in Figure IV-6.

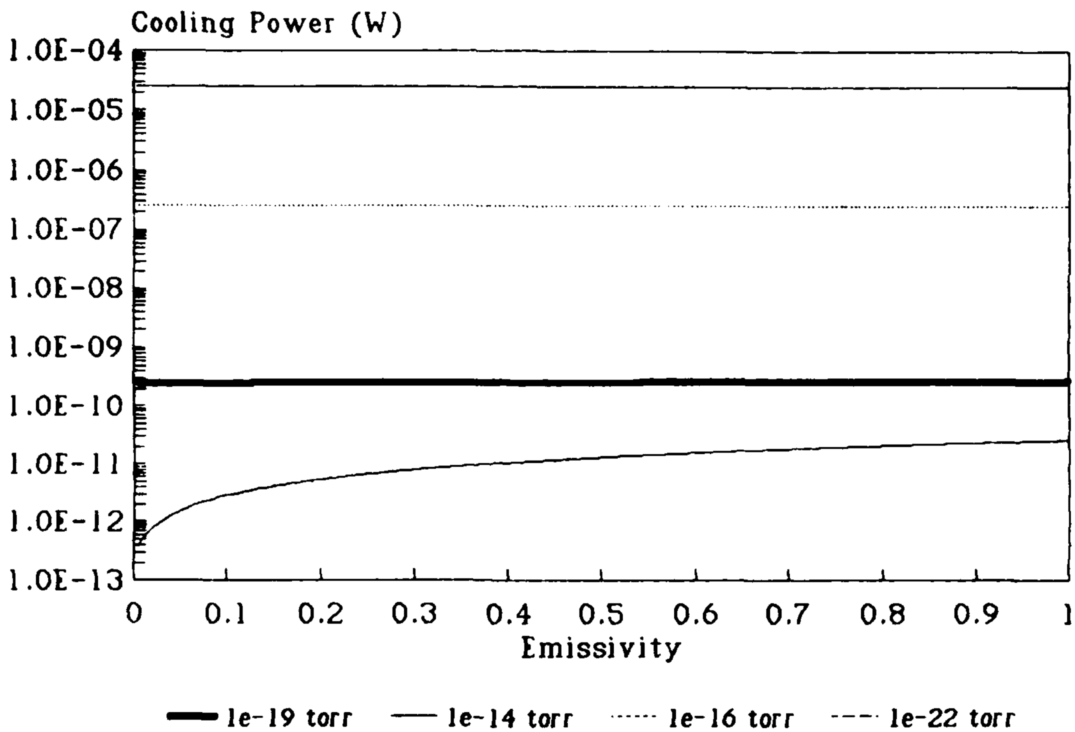

Figure IV-6. Cooling Power Requirement at Various Emissivities

7 Effect of Wall Thickness

Wall thickness becomes more important at higher pressures, when annihilation energy is the dominant contributor to cooling power. The effect is not large at the pressures and thicknesses considered here, however, as shown in Figure IV-7. It is not apparent in the figure, but the curves are linear at all pressures, indicating that 3 cm is much less than the interaction lengths of the annihilation radiation.

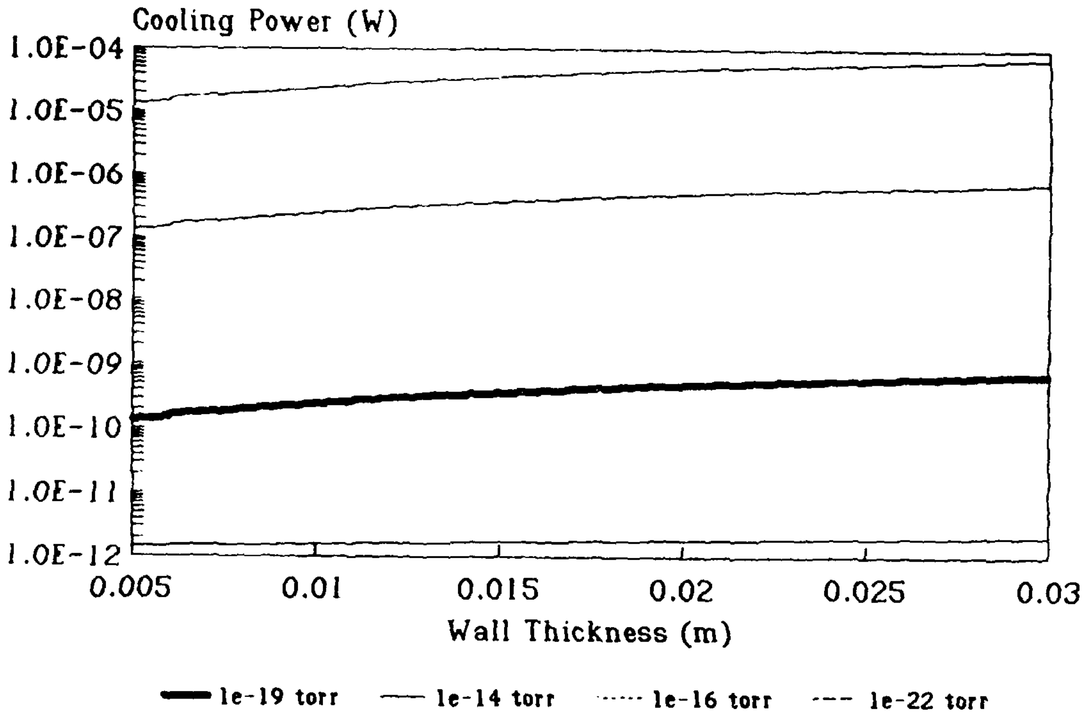

Figure IV-7. Cooling Power Requirement for Various Wall Thicknesses

V <u>Analysis and Conclusion</u>

It may be possible to store antimatter in the manner discussed in this study, but too many issues remain open to make a definitive judgement one way or the other. Subject to the many explicit and implicit assumptions made, it may be possible to store useful quantities of antimatter in the manner discussed without exceeding the cooling-power limits of present cryogenic techniques. However, there are problems with the assumptions, some of which are highlighted below.

For the most part, all of the pressure levels discussed are below the measurable limit of 10^{-14} torr. It is by no means a given that such pressures can be sustained. Even should the required temperatures and number densities be reached, the concept of pressure may not be applicable in the sense in which it is used here: that is, the Maxwell-Boltzmann distribution and the ideal gas law might not apply. The question of just where the gas in the vacuum chamber comes from is also left open. It would be reasonable to think that any hydrogen gas in the system got there by sublimation from the chamber wall. Were this the case, however, there would be a similar sublimation rate from the antihydrogen sphere, and disaster might be near. Perhaps also ^3He from the cooling bath outside the chamber wall would be the more likely gas to appear in the system.

The assumption that the antihydrogen was entirely in the para state has significant impact on the results, and may turn out to be ill-founded. Parahydrogen has very different physical properties from orthohydrogen, including density, thermal conductivity, vapor pressure, and phase-change temperatures and enthalpies.

Orthohydrogen also is a significant source of stored energy at low temperatures, since it releases a large amount of energy (520 J/g or 0.011 eV/molecule) when it converts to parahydrogen. This is comparable to the energy deposited per molecule by a charged pion from a proton-antiproton annihilation, as shown by equation (19) in Section II. If the process by which antihydrogen may someday be solidified (a crucial assumption in itself) turns out to produce an end product with significant concentrations of anti-orthohydrogen, this analysis would certainly have to be redone to include the effects of the mixed substance.

The assumptions that the ice ball has a single temperature and that no sublimations occur are also suspect. There are several related problems in this area. First, more analysis needs to be done on the process of energy deposition by charged pions in solid hydrogen. The possibility remains that pions will cause local sublimation of hydrogen molecules. Second, since the impulse response time of the hydrogen may be comparable to the annihilation rate, hot paths within the ice ball may overlap. Since the warmer regions are more conductive, heat may be concentrated at impact points on the surface, where sublimation could occur into the chamber. Third, the question of shock effects on the ice ball from annihilations has been ignored. Finally, the hydrogen vapor pressure curve used was fit to data points which must themselves have been extrapolations; its accuracy may be poor.

The cooling-power requirements of storing solid antimatter for extended times may not be an obstacle, if the proper conditions obtain. However, whether these conditions are indeed possible remains in doubt. Many difficult questions remain to be answered before it can be stated that the goal of long-term storage is or is not within the reach of present cryogenic technology.

Bibliography

1. Robert L. Forward, Antiproton Annihilation Propulsion, pp. 119-128. AFRPL TR-85-034, September, 1985.

2. J. T. Bahns (ed.), Proceedings of the Cooling, Condensation, and Storage of Hydrogen Cluster Ions Workshop, Dayton, Ohio, 8-9 January 1987.

3. Robert D. McCarty, *Hydrogen: Its Technology and Implications*. CRC Press, Cleveland, p. 195 (1975).

4. O. V. Lounasmaa, *Experimental Principles and Methods Below 1K*. London, Academic Press, p. 67 (1974).

5. W. Thompson and S. Hanrahan, "Characteristics of a cryogenic extreme high-vacuum chamber." *J. Vac. Sci. Technol.* 14, 643 (1977).

6. Y. S. Touloukian and D. P. DeWitt, Thermal Radiative Properties: Metallic Elements and Alloys. *Thermophysical Properties of Matter*, vol. 7, IFI/Plenum, New York, p. 1212 (1970).

7. Robert Siegel and John R. Howell, *Thermal Radiation Heat Transfer (2nd ed.)*. New York, Hemisphere, p. 241 (1981).

8. G. F. Weston, *Ultrahigh Vacuum Practice*. London, Butterworths, p. 4 (1985).

9. Robert L. Forward, Antiproton Annihilation Propulsion. AFRPL TR-85-034, p. 111 (1985).

10. James R. Gaines (University of Hawaii, Honolulu), "Energy Deposition in Solid H_2 due to Proton-Antiproton Annihilation." Unpublished preprint (1988).

11. Particle Data Group, Review of Particle Properties. *Rev. Mod. Phys.* 56, S56 (1984).

12. Randall Barron, *Cryogenic Systems*, New York, McGraw-Hill, p. 28 (1966).

13. P. W. Atkins, *Physical Chemistry*. W. H. Freeman, New York, p. 774 (1986).

14. Isaac F. Silvera, "The solid molecular hydrogens in the condensed phase: Fundamentals and static properties." *Rev. Mod. Phys.* 52, 393-452 (1980).

15. Leslie L. McKee and James A. Lupo, *The Physics of Charged Particle Beams*, Air Force Institute of Technology staff notes for PHYS 7.54, p. 2-4 (1987).

16. James E. Turner, "Stopping Powers and Ranges of Charged Particles," *Hand book of Radiation Measurement and Protection*, Sect. A, Vol. 1, Allan Brodsky, ed., pp. 213-228. CRC Press, West Palm Beach, FL (1978).

17. Richard Haberman, *Elementary Applied Partial Differential Equations*, Prentice-Hall, Englewood Cliffs, NJ, p. 412 (1987).

18. Isaac F. Silvera, "The solid molecular hydrogens in the condensed phase: Fundamentals and static properties." *Rev. Mod. Phys.* 52, 393-452 (1980).

19. Walter H. Barkas and Martin J. Berger, Tables of Energy Losses and Ranges of Heavy Charged Particles. NASA SP-3013, p. 108 (1964).

20. Isaac F. Silvera, The solid molecular hydrogens in the condensed phase: Fundamentals and static properties. Rev. Mod. Phys. 52, 393-452 (1980).

Vita

Captain Michael J. MacLachlan [redacted] in 1976 [redacted] attended Webster College in Saint Louis, Missouri, from which he received the degree of Bachelor of Music in vocal performance in 1980. After undertaking some graduate work in music at Indiana University and engineering studies at Southern Illinois University, Roosevelt University, the University of Chicago, and Saint Louis University, he attended Officer Training School and received a USAF commission in 1982. His first assignment was to the Air Force Institute of Technology, which awarded him the degree of Bachelor of Science in Electrical Engineering in March 1984. He was then assigned to NASA Johnson Space Center, where he worked for USAF Space Division in the Shuttle Operations and Planning Complex Project Office. In 1987, Captain MacLachlan was reassigned to AFIT to obtain the degree of Master of Science in Nuclear Engineering. Upon graduation in March 1989, he will be assigned to Air Force Logistics Command at Hill AFB, Utah.